ACS OMEGA

http://pubs.acs.org/journal/acsodf

Article

Combustion Behavior and Thermal Degradation Properties of Wood Impregnated with Intumescent Biomass Flame Retardants: Phytic Acid, Hydrolyzed Collagen, and Glycerol

Luming Li, Zhilin Chen, Jinhan Lu, Ming Wei, Yuxiang Huang, and Peng Jiang*

Cite This: *ACS Omega* 2021, 6, 3921−3930

Read Online

ACCESS | Metrics & More | Article Recommendations

ABSTRACT: Wood is a natural renewable material with a porous structure widely used in construction, furniture, and interior decoration, yet its intrinsic flammability poses safety risks. Therefore, environmentally friendly flame retardants have received increasing attention. In this study, a water-soluble flame retardant, consisting of bio-resourced phytic acid (PA), hydrolyzed collagen (HC), and glycerol (GL), was used to improve the flame retardancy of wood ("PHG/wood") through full cell vacuum-pressure impregnation. Morphology and Fourier transform infrared analysis results show that the flame retardant impregnated the wood and adhered evenly to the wood vessels. A PA/HC/GL ratio of 3:1:1 (concentration of the flame retardant solution = 30%) maximized the limiting oxygen index (LOI, 41%) and weight gain (51.32%) for PHG-C30/wood. The flame retardant formed an expansive layer after heating, and the treated wood showed an improved combustion safety performance such that the fire performance index and residue of PHG-C30/wood were 75 and 126.8% higher compared with that of untreated wood, respectively. The peak and total heat release were also significantly reduced by 54.7 and 47.7%, respectively. The PHG/wood exhibited good carbon-forming performance and a high degree of graphitization after combustion. The dense carbon layer provides condensed phase protective action, and non-combustible volatile gases, such as H_2O, CO_2, and NH_3, are released simultaneously to dilute the fuel load in the gas phase. Thus, PHG is shown to be an effective flame retardant for wood.

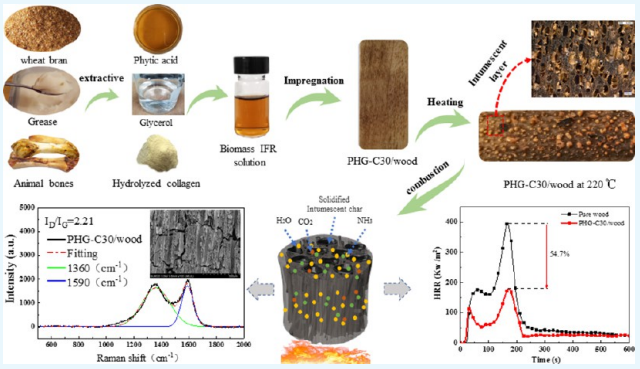

INTRODUCTION

Wood is a natural and stable material with favorable aesthetic qualities and sustainability credentials. Wood is therefore widely used in furniture, as a decorative material, and for residential building construction.[1,2] However, as a material with a porous structure primarily composed of cellulose, hemicellulose, and lignin, wood is inherently combustible, producing hydrocarbons and combusting at <300 °C.[3] The low fire safety of wood often results in unwanted fires and can cause injuries or fatalities. To address this, flame retardant treatments are a useful strategy. Various flame retardants have been successfully developed to reduce combustibility and can be categorized into halogen-containing and halogen-free flame retardants.[4] However, halogen-containing materials produce toxic gases during the combustion process (e.g., dioxin). Recently, due to environmental and health concerns, the application of this category of flame retardants has been increasingly avoided or banned in European countries and the United States of America.[5] Furthermore, most flame retardant operations depend heavily on exhaustible fossil resources, which is not conducive to sustainable development. In response, new flame retardant solutions, developed using bio-based materials and renewable resources, have attracted increasing interest as more sustainable, widely available, and environmentally friendly alternatives.[6−8]

Intumescent flame retardant (IFR) systems are efficient at limiting combustion by producing a swollen multicellular char capable of protecting the treated material from flames.[9] Wood has a naturally porous structure that can be used as a micro reaction vessel, suitable for flame retardants to enter, and its structure provides abundant conduits for effective impregnation.[10] When heated, IFR decomposes, producing an expanded carbon layer covering the inside of the impregnated space and blowing out of the surface in the case of wood, which has a protective effect. Phytic acid (PA) is a natural substance

Received: November 27, 2020
Accepted: January 21, 2021
Published: January 29, 2021

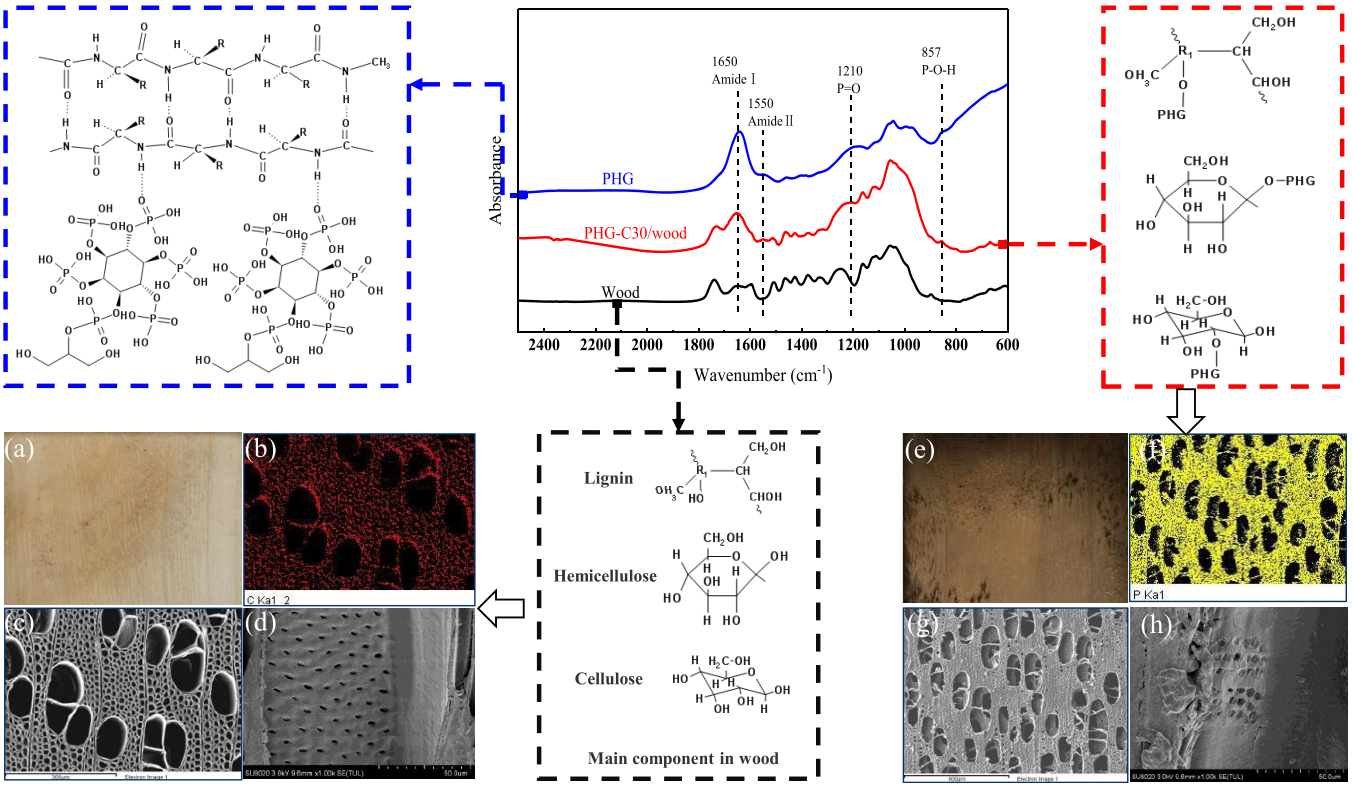

Figure 1. Infrared spectrum of pure (untreated) wood, PHG, and PHG-C30/wood and their morphologies and elemental mapping: (a) digital image of pure wood and (e) PHG-C30/wood; (b) EDX spectra of pure wood showing an abundance of C and (f) PHG-C30/wood showing the presence of P due to the impregnation of the PHG-C30 solution; (c) SEM image of a cross section in pure wood (300-μm scale) and (d) wood vessels in a longitudinal section (50-μm scale) showing smooth and clean pits; (g, h) SEM images of a cross section in PHG-C30/wood (600 μm scale) and wood vessels in a longitudinal section (50 μm scale) showing fillers and membranous substances.

extracted from seeds, grains, and legumes, and it is a sustainable, environmentally friendly, and non-toxic organic compound containing P. The six phosphate groups in the molecular structure of PA yield strong chelating properties.[11] Furthermore, upon exposure to a flame or heat flux, PA can form phosphoric acid, which favors the dehydration of cellulosic substrates and forms a stable protective char.[12] PA has been used as a flame retardant for coatings, cotton, wool fabrics, polylactic acid, and epoxy resins.[13−17] Collagen is one of the main proteins forming an extracellular matrix[18] and is regarded as one of the most useful biomaterials. Excellent biocompatibility, safety, and biodegradability make collagen a primary resource in medical applications.[19] Collagen is an environmentally friendly non-toxic material that contains various amino acids rich in N and other elements that may provide good flame retardant effects. Studies have shown that after heating, collagen can form non-flammable gas[20] and act as a flame retardant. Moreover, intense electrostatic attraction may occur between various collagen-containing amino acids and other eco-friendly bio-based compounds, including PA,[13] thus forming a greener P−N flame retardant system.

The aim of this study is to explore a novel biomass flame retardant system for wood. We selected bio-based PA as an acid source, hydrolyzed collagen (HC) as a blowing agent, and glycerol (GL), which is mutually soluble with PA and improves the carbonization performance of wood, to prepare an IFR aqueous solution. Following full cell vacuum-pressure impregnation, the environmentally friendly flame retardant wood was prepared. The morphology, thermal stability, and combustion behavior of the treated wood were investigated along with the flame retardant mechanism of the condensed and gas phases. This environmentally friendly flame retardant system provides new approaches for the sustainable and simple flame retardant treatment of wood.

RESULTS AND DISCUSSION

Morphology and Characterization. By observing the morphology and elements after impregnation, the distribution of PHG in the wood structure was visualized. Figure 1a−h shows the scanning electron microscopy−energy-dispersive X-ray (SEM−EDX) observations of PHG-C30/wood (treated with PHG-C30) in comparison to those of pure (untreated) wood. The pure wood (Figure 1a) has a clean surface, the original color of wood, and its EDX energy spectra show a high C content (Figure 1b). The SEM micrograph of the cross section shows the porous structure of the wood (Figure 1c). The larger oval-shaped holes are the pores of the vessel, while the smaller holes are the pores of the wood fibers. All pores are smooth and free of foreign matter. Microscopic pores (called "pits") in the longitudinal section SEM image of the vessels (Figure 1d) act as pathways for the exchange of substances within the wood cells and are well aligned with a clear morphology and smooth channels. In comparison, the PHG-C30/wood samples showed notable differences: the surface of the treated wood was darker (Figure 1e) as the phosphate group in PA has a high acidity and oxidization ability, which destroys the cellulose and hemicellulose structures in wood.[10] The EDX spectrum of the treated wood (Figure 1f) shows the presence of a large amount of P, indicating that the PHG-C30 had entered the wood interior. The SEM images (Figure 1g,h)

https://dx.doi.org/10.1021/acsomega.0c05778
ACS Omega 2021, 6, 3921−3930

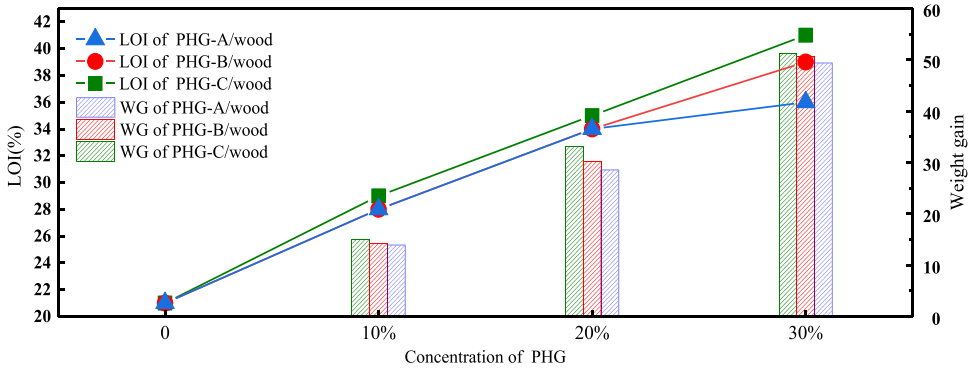

Figure 2. Weight gain (WG) and LOI values of the PHG-treated wood samples at different treatment concentrations.

show that the pores of the wood fiber became smaller, less smooth, and appeared more compact,[22] which reflect the attachment of the fillers (PHG-C30) inside the pores. Furthermore, the inner walls of the pores appeared to be covered by a membranous substance, which partially obscured their underlying morphology. Overall, these differences indicated that the PHG-C30 flame retardant had impregnated the wood and adhered evenly to the wood vessels.

The Fourier transform infrared (FTIR) spectra of the pure wood, PHG, and PHG-C30/wood further verify these changes (Figure 1). Specifically, the peaks identified in the PHG and PHG-C30/wood at approximately 1650 and 1550 cm^{-1} correspond to the characteristic bands of amide I (C═O stretching) and amide II (N−H bending and C−N stretching)[23] in HC, respectively. Compared with the spectrum of pure wood, the spectra of the PHG-C30/wood samples displayed new bands at 1210 cm^{-1} corresponding to the stretching vibration of P═O[24] and 857 cm^{-1} corresponding to the stretching vibration of P−O−H,[25] which are structures attributed to PA. The signals of GL were difficult to distinguish from those of the wood because of their similar chemical structures (i.e., C and −OH). Nevertheless, a peak near 1037 cm^{-1} was attributed to GL.[26]

Fire Safety Properties of PHG/Wood. *Combustion Behavior Analysis.* Figure 2 shows the weight gain (WG) and limiting oxygen index (LOI) of the different samples. The WG of the PHG loaded in the wood sample was calculated as follows:

$$W(\%) = (M_2 - M_1)/M_1 \times 100\%, \quad (1)$$

where M_1 is the mass of the wood sample (g) and M_2 represents the mass of the wood sample after PHG impregnation (g).

As the PHG concentration increased, the WG of the treated wood increased. For the same PHG concentration, the WG of the PHG-C/wood was higher than that of the PHG-B/wood and PHG-A/wood samples. When the PHG concentration was 30%, the WG of the PHG-A30/wood, PHG-B30/wood, and PHG-C30/wood was 49.37, 50.68, and 51.32%, respectively. As the increase in PHG concentration is mainly due to the increase in PA components, PHG-C > PHG-B > PHG-A for the WG, which is mainly due to the enhanced permeability of PA; the increase in the PA concentration is conducive to the entry of PHG components into the wood.[27] In comparison to the LOI of pure wood (21%), the LOI of PHG-A/wood, PHG-B/wood, and PHG-C/wood increased with the PHG concentration. Additionally, at the same PHG concentration, the LOI of the PHG-C/wood samples was always higher than that of the other two sample types; at a PHG concentration of 30%, the LOI of the PHG-A30/wood, PHG-B30/wood, and PHG-C30/wood samples was 36, 39, and 41%, respectively, indicating an increase of 71.4, 85.7, and 95.2%, respectively, compared to that of pure wood. This phenomenon shows that with an increase in the PHG concentration, the flammability of wood is effectively improved; this also shows that PHG has a good flame retardant effect.

CONE is applied in the bench-scale assessment of fire parameters and is considered an effective means of simulating actual fire-burning behaviors.[28] During the test, the following parameters were determined: heat release rate (HRR), total heat release (THR), total smoke release (TSR), smoke production rate (SPR), and residual mass. Table 1 lists the corresponding data, which are shown in Figure 3.

Table 1. CONE Data for the Pure Wood and PHG-C/Wood Samples[a]

sample	FPI (TTI/pHRR)	pHRR (KW/m^2)	THR (MJ/m^2)	TSR (m^2/m^2)	pSPR (m^2/S)	residue (wt %)
pure wood	0.048	394.2	53.9	253.9	0.020	3.7
PHG-C10/wood	0.059	185.4	40.7	40.9	0.004	20.4
PHG-C20/wood	0.082	182.1	32.4	40.0	0.001	21.2
PHG-C30/wood	0.084	178.5	28.2	64.0	0.006	22.1

[a]FPI: fire performance index; pHRR: peak of heat release rate; THR: total heat release; TSR: total smoke release; pSPR: peak of smoke production rate.

The fire performance index (FPI = TTI/pHRR) is an important parameter for the characterization of fire safety, where higher FPI values indicate higher fire safety.[29] The FPI of the PHG-C30/wood was 75% higher than that of pure wood, which indicates a lower combustion risk. Figure 3a shows that the combustion of all samples can be divided into two stages.[30] The pHRR and THR values of pure wood were 394.2 kW/m^2 and 53.9 MJ/m^2, respectively; only 3.7% remained as char residue. For the PHG-C30/wood samples, the pHRR and THR values were 178.5 kW/m^2 and 28.2 MJ/m^2, respectively, which are 47.7 and 54.7% lower than those of pure wood. Figure 3c,d shows the difference in the smoke emissions between the treated and untreated wood. The TSR

https://dx.doi.org/10.1021/acsomega.0c05778
ACS Omega 2021, 6, 3921−3930

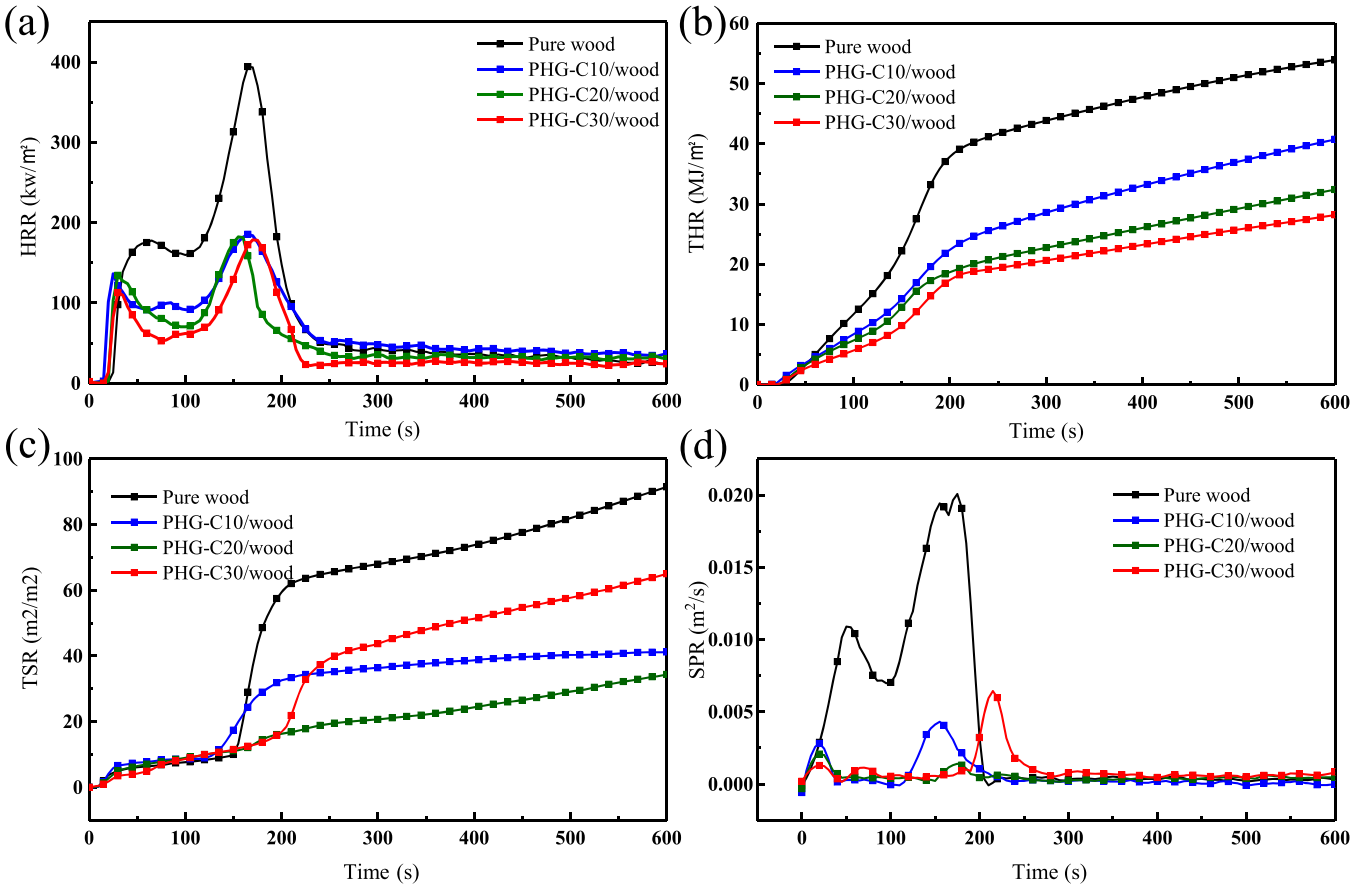

Figure 3. (a) HRR, (b) THR, (c) TSR, and (d) SPR of the pure wood and PHG-C/wood samples.

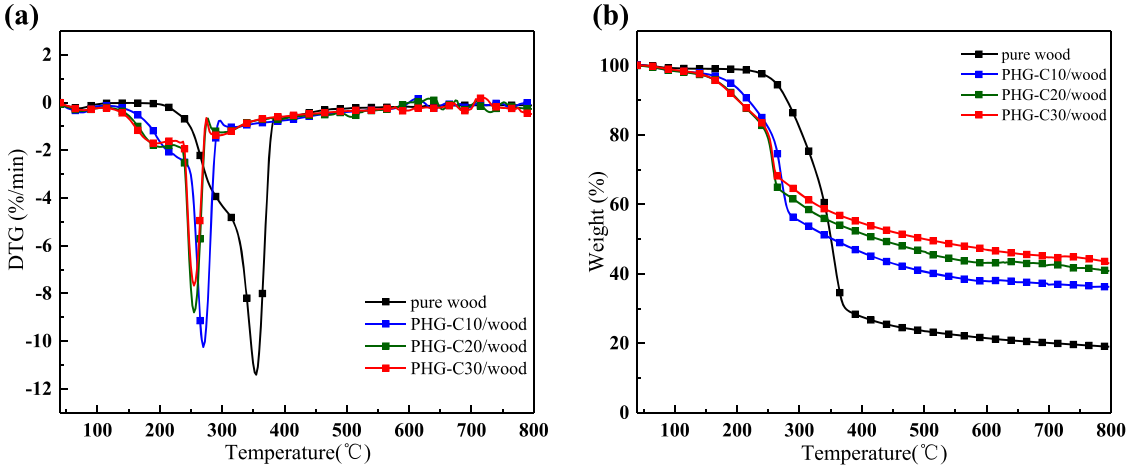

Figure 4. (a) TGA and (b) DTG curves for pure wood and PHG-C/wood.

and pSPR values of the PHG-C/wood samples were significantly lower than those of the pure wood. The TSR value of the PHG-C20/wood sample was the lowest at 40 m^2/m^2, which was 15.75% lower than that of pure wood; the pSPR was 0.001 m^2/s and 5% of the value for wood, which were lower than those of the PHG-C10/wood and PHG-C30/wood samples. Furthermore, at the end of the experiment, the final char residue of PHG-C30/wood was 22.1%, which was approximately sixfold higher than that of pure wood. These results show that PHG/wood provided a higher fire safety standard than pure wood.

Thermal Degradation Performance. Figure 4 shows the TGA and derivative thermogravimetry (DTG) curves (performed in N) of the samples, and the corresponding data are presented in Table 2. For the pure wood, the DTG curves (Figure 4a) show two notable stages: water evaporation and main pyrolysis. The first degradation stage occurred from 40 to 120 °C with a maximum mass loss rate at 67 °C (Table 2) due to the release of moisture from the moisture absorption of wood during storage and experiments.[31] The main pyrolysis process occurred from approximately 220 to 450 °C. During this stage, the mass loss was mainly the result of cellulose and hemicellulose decomposition,[32] and the temperature at the

https://dx.doi.org/10.1021/acsomega.0c05778
ACS Omega 2021, 6, 3921−3930

Table 2. TGA Data for Pure Wood and PHG-C/Wood[a]

sample	$T_{5\%}$ (°C)	T_{max} (°C) stage 1	T_{max} (°C) stage 2	R_{max} (%/°C) stage 1	R_{max} (%/°C) stage 2	residues (800 °C wt %)
pure wood	260	67	355	0.24	11.41	19.0
PHG-C10/wood	187	72	269	0.41	10.24	36.3
PHG-C20/wood	172	75	254	0.36	8.79	40.8
PHG-C30/wood	170	77	255	0.31	7.67	43.1

[a] $T_{5\%}$: temperature at 5% weight loss; T_{max}: temperature at the maximum weight-loss rate; R_{max}: maximum decomposition rate.

maximum weight-loss rate was 355 °C. Corresponding to the DTG results, the TGA curve (Figure 4b) shows that the devolatilization process began at approximately 40 °C and proceeded rapidly with increasing temperature until approximately 450 °C, after which the weight decreased slowly to the end of the test with a 19% residue.

For the PHG-C/wood samples, although the curves in Figure 4 also show that pyrolysis could be divided into two stages (i.e., water loss and main degradation) and the degradation trend was similar to that of pure wood, the pyrolysis behavior of the PHG-C/wood samples was significantly different during the two stages (Table 2). When heating started, the mass change was small with increasing temperature; therefore, we selected $T_{5\%}$ as the initial temperature of decomposition.[33] The initial decomposition temperature ($T_{5\%}$) of PHG-C10/wood (187 °C) was 73 °C lower than that of pure wood (260 °C). When the concentration of PHG-C increased, $T_{5\%}$ showed a gradually decreasing trend, which indicated that the flame retardant decomposed earlier than wood during the initial combustion stage. This is consistent with observations of the changes in the morphology of the pure wood and PHG-C30/wood (Figure 1). During the first stage (water loss), the T_{max} and R_{max} of PHG-C/wood were higher than those of pure wood. This indicates that PHG/wood had a higher evaporation rate during the first stage but also required more heat. These data indicate that PHG flame retardants promote heat absorption and thus accelerate the evaporation of water.

During the second stage (main degradation), the T_{max} and R_{max} of PHG-C/wood were opposite to those of the first stage, both being lower than those of pure wood, and the R_{max} of PHG-C30/wood was 32.78% lower than that of pure wood at 7.67%/°C. These observations indicate that the decomposition of the treated wood was notably reduced. The T_{max} of PHG-C30/wood was 255 °C, which was 100 °C lower than that of pure wood. This decrease in T_{max} strongly suggests that the flame retardant reacted before the wood began to decompose. The main period of weight loss occurred during the second stage of PHG-C/wood combustion due to the cleavage of

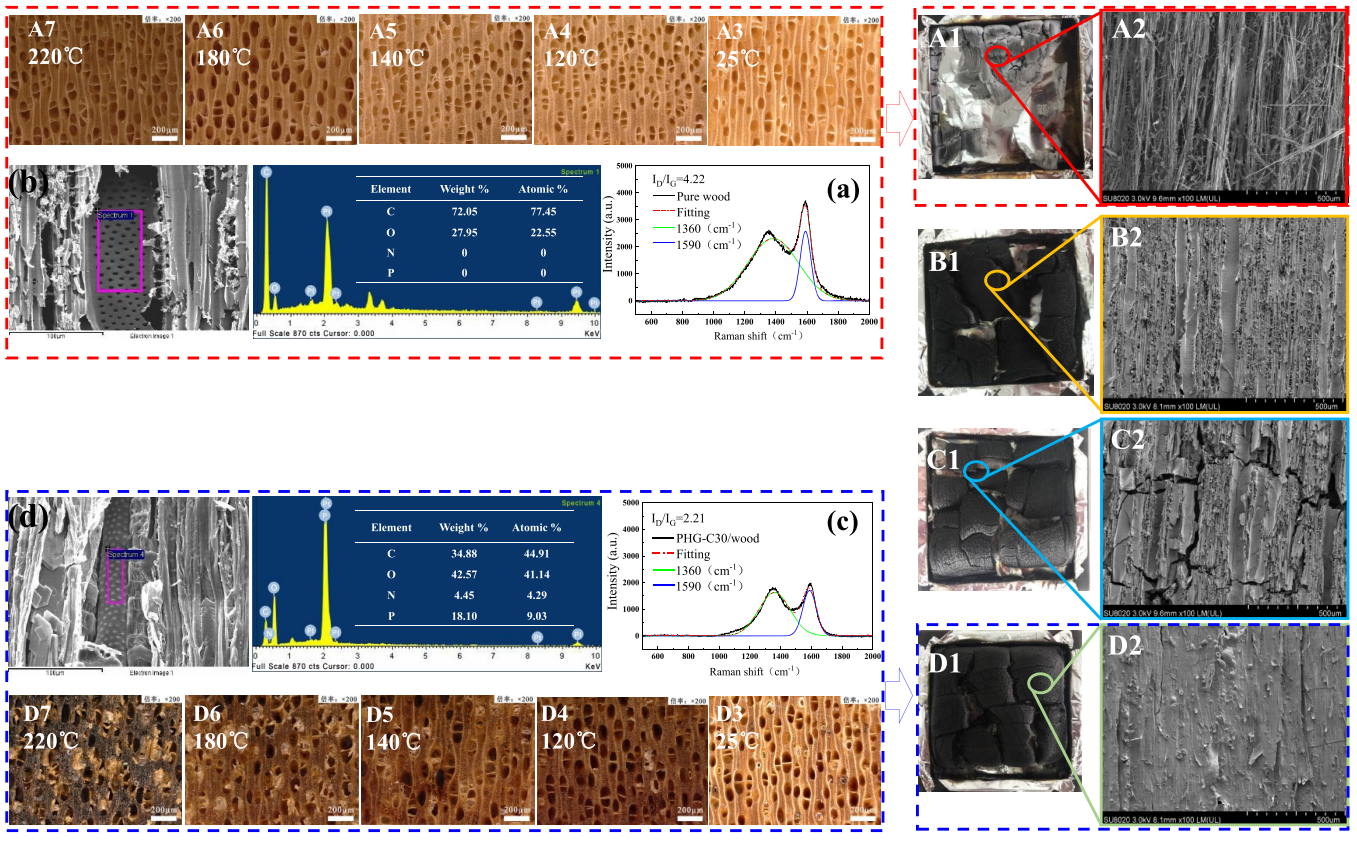

Figure 5. Char residues after the CONE tests (A1: pure wood, B1: PHG-C10/wood, C1: PHG-C20/wood, and D1: PHG-C30/wood) and corresponding SEM micrographs (500 μm scale; A2, B2, C2, and D2) showing an increasing proportion of C residue. (a) Pure wood and (c) PHG-C30/wood C residue Raman peak fitting curves indicating that the char of PHG-C30/wood had a higher degree of graphitization. (b) Pure wood and (d) PHG-C30 /wood C residue EDX spectrometry showing that the char of PHG-C30/wood had a high P content; (A3–A7) morphological changes in the pure wood and (D3–D7) PHG-C30/wood at different temperatures (25, 120, 140, 180, and 220 °C), where PHG-C30/wood shows a notable foaming/expansion effect.

https://dx.doi.org/10.1021/acsomega.0c05778
ACS Omega 2021, 6, 3921−3930

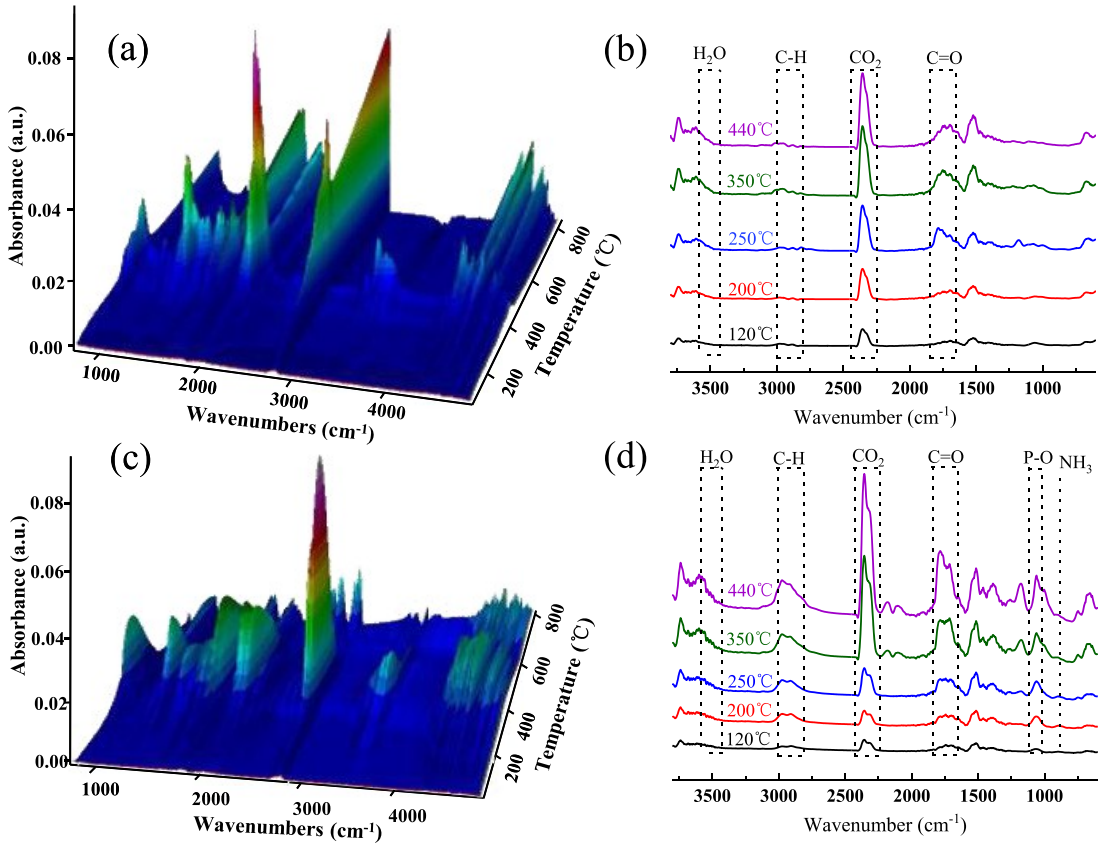

Figure 6. Three-dimensional FTIR-TGA spectra of pyrolysis volatiles and the corresponding FTIR spectra under different temperatures for (a, b) pure wood and (c, d) PHG-C30/wood.

peptide bonds and the degradation of the side chain groups in the amino acid residues of the HC.[34] Thus, the heat absorbed by the PHG flame retardant provided effective protection of the wood substrate. When the temperature reached 800 °C (the experimental end point), the C residue increased significantly with PHG treatment. The C residue of pure wood was 19.0%, while that for the PHG-C30/wood was 43.1%, which indicated an increase of 126.8%.

Mechanism Analysis. *Char Analysis.* The protective layer of C produced by the burning of a material prevents fire from further combustion.[35] The C morphology formed at the beginning of heating and the char residues for pure wood and PHG-C/wood after the CONE tests were further investigated (Figure 5). For this, morphological changes in the PHG-C30/wood and pure wood samples were examined at different temperatures (25, 120, 140, 180, and 220 °C). This showed that the surfaces of pure wood (Figure 5A3−A7) experienced negligible changes beyond the gradual darkening that is typical of heat-treated wood.[36] Up to 220 °C, the surface of the pure wood was clean, and no expansion materials were produced. However, under the same conditions, above 120 °C, the surface of the PHG-C30/wood samples gradually produced an expanded foaming layer, and their color became significantly darker (Figure 5D3−D7). At 220 °C, the surfaces of the treated wood were covered by an expanded layer with a distinct foaming/expansion effect.

From the char residues after the cone tests (Figure 5A1) and the corresponding SEM image (Figure 5A2), negligible residue remained on the pure wood, and the C residue was loose. However, after the PHG-C/wood burned, the residue was relatively complete, and larger block carbonization was retained (Figure 5B1−D1). With an increase in the PHG-C concentration, the amount of C residue also increased. The carbonization residue of PHG-C30/wood (Figure 5D1,D2) was the most complete and intact, forming a dense surface cover. Yang et al.[37] introduced, in detail, the flame retardant mechanism of the C layer in the condensed phase, which can also explain the flame retardancy of wood materials. The dense char layer can better isolate the underlying wood matrix from the air, and thus preventing heat transfer and the emission of the flammable gas mixtures.

Raman spectra and EDX of the char were used to analyze the flame retardant mechanism in the condensed phase. The I_D/I_G ratio can be used to indicate the degree of graphitization of char[38] with peaks at approximately 1360 and 1590 cm^{-1} attributed to the D band and G band, respectively. The I_D/I_G value of pure wood was 4.22 (Figure 5a) compared to 2.21 for PHG-C30/wood (Figure 5c), indicating a higher degree of graphitization for the treated wood char, which means a more restrained effect in heat and mass diffusion during combustion.[33] In contrast, the EDS spectra of pure wood and PHG-C30/wood C residues (Figure 5b,d) show that the P-containing compounds in the char that formed in the flame retardant wood were very high. This is attributed to the accumulation of P-containing compounds on the surface of the char layer, which helps improve the completeness of the char.[39] Importantly, the high completeness of the C layer prevents the exchange of heat and flammable gas, thus effectively preventing combustion.

https://dx.doi.org/10.1021/acsomega.0c05778
ACS Omega 2021, 6, 3921−3930

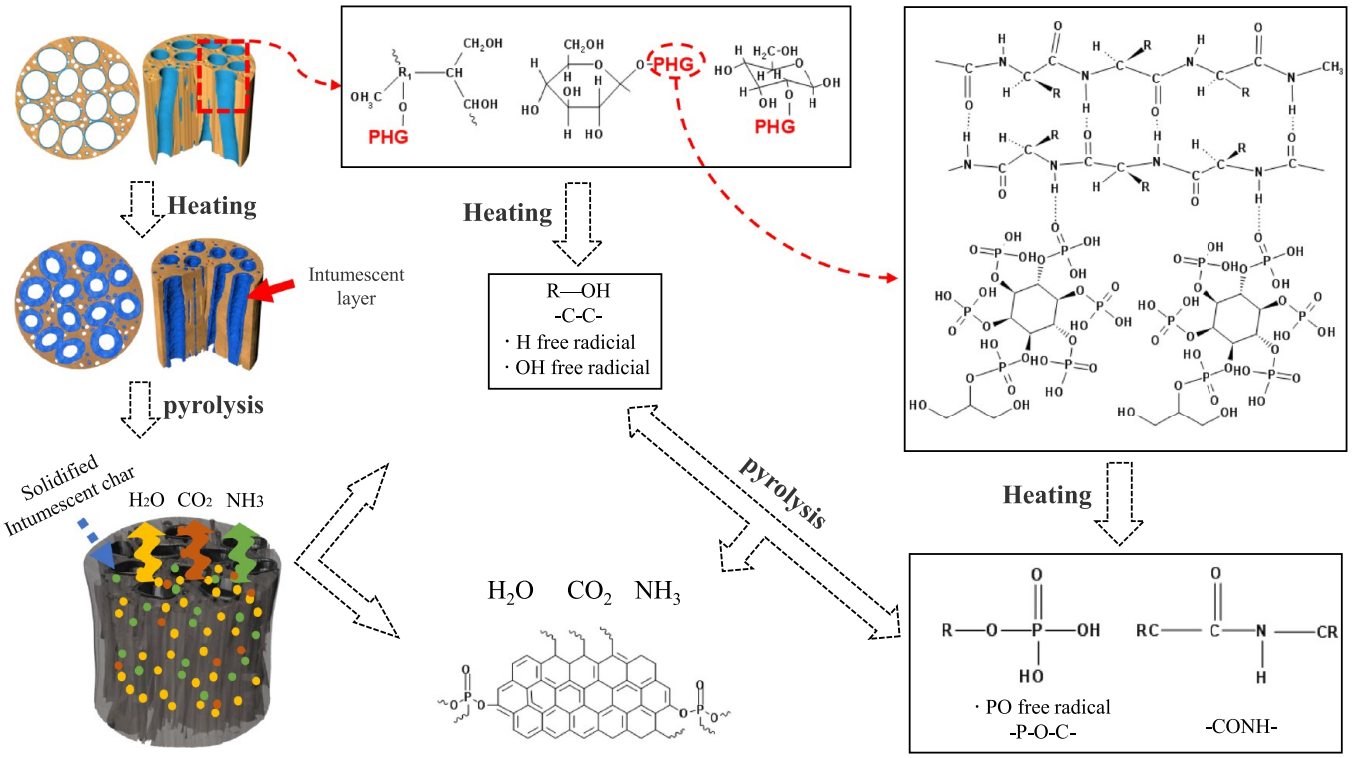

Figure 7. Proposed model of the flame retardancy mechanism for PHG-treated wood.

FTIR-TGA Analysis. FTIR-TGA was used to explore the gas phase of the pure wood and PHG-C30/wood during thermal decomposition. Figure 6a,c shows three-dimensional images of the evolved gaseous products for these samples, and Figure 6b,d shows the FTIR spectra of the gases released at 120, 200, 250, 350, and 440 °C. These temperatures were chosen according to the DTG curves presented in Figure 4a and correspond to the temperatures at which maximum degradation occurred. For the pure wood (Figure 6a,b), there were few differences in the characteristic peaks of the main degradation products, except for the intensity of each peak. The absorption bands at approximately 2350 and 1730 cm^{-1} were assigned to CO_2 and C═O, respectively;[40] the peak at approximately 2910 cm^{-1} corresponded to C−H, which was attributed to hydrocarbons; and the peak at approximately 3500 cm^{-1} was ascribed to H_2O. For the PHG-C30/wood samples (Figure 6c,d), the H_2O, C−H, CO_2, and C═O peaks were also present; however, a new absorption peak also appeared near 915 cm^{-1}, which was assigned to the characteristic absorption peak of NH_3.[41] The peak near 1080 cm^{-1} was assigned to P−O groups,[42] which is capable of scavenging highly active $H^{\cdot}$ and $HO^{\cdot}$ radicals, thus inhibiting combustion in the gas phases.[43] The presence of ammonia and P-containing gas can therefore be attributed to the decomposition of PHG-C30. This demonstrates the important role of PHG-C30 in gas-phase flame retardation.

Flame-Retardancy Mechanism. Based on the analysis of the char and FTIR-TGA, a possible mechanism for the flame retardant behavior of the modified wood was developed, as shown in Figure 7. According to the model, when the sample is heated or on fire, the PHG flame retardant first decomposes and releases a large amount of non-combustible gases, such as H_2O, CO_2, P−O groups, and NH_3. These non-flammable gases dilute flammable gas and O in the surrounding air and remove heat.[44] At the same time, P−O groups scavenge highly active $H^{\cdot}$ and $HO^{\cdot}$ radicals. The PA catalyzes GL and the primary composition of wood to dehydrate and carbonize, forming an intumescent char layer in the porous structure of the wood, which can act as a barrier to effectively limit heat transfer.[45] Thus, by terminating activity in the gas phase and forming a carbonaceous layer, the combustion process can be interfered,[46] and the underlying substrate is protected from further thermal decomposition.

CONCLUSIONS

The combustion properties of wood treated with a biomass-derived PA, HC, and GL IFR were experimentally observed. The WG and LOI significantly increased following the treatment. PHG-C30/wood had the highest WG (51.32%) and LOI (41%). Furthermore, based on morphological changes before and after PHG treatment, the flame retardant effectively penetrated the wood, decomposed first when heated, and produced an expanded foaming layer that played a role in protecting the wood during combustion. The TGA and CONE results showed that the amounts of residues in the PHG-treated wood were significantly higher than those for untreated wood; PHG-treated wood was decomposed by heat earlier than pure wood, which protected the inner wood matrix. The FPI also showed that the treated wood had a higher degree of fire safety. The maximum pyrolysis rate (R_{max}) of the PHG-C30/wood samples was 32.78% lower than that of pure wood, the THR was 47.7% lower, and the pHRR was reduced by 54.7%. In addition, the TSR and SPR were also significantly reduced. The flame retardant mechanism analysis revealed that the P-containing group accumulated by the PHG-C30/wood in the condensed phase C layer improved the C completeness and degree of graphitization of residual C and established a combustion barrier while the continued burning

https://dx.doi.org/10.1021/acsomega.0c05778
ACS Omega 2021, 6, 3921−3930

of PHG-C30/wood released H_2O, CO_2, NH_3, and P−O groups in the gas phase combustion. These effects can dilute the air and prevent the continuous combustion chain reaction.

MATERIAL AND METHODS

Materials. Poplar (*Populus girinensis* Skv.) acquired in Hebei Province, China, was used as the wood material. The moisture content was approximately 10%, and the air-dried density was 0.40 g/cm^3. As a flat-sawn board, the wood sample size was 200 × 150 × 20 mm, and all sides were plain. PA (70% aqueous solution) was supplied by Sinopharm Chemical Reagent Co. Ltd., China; HC was supplied by Shijiazhuang Xuermei Biological Technology Co. Ltd., China; and GL was supplied by Beijing Jintongletai Chemical Products Co. Ltd., China.

Table 3. Sample Number, Dosages of Each Component, and Flame Retardant Concentration

samples		PA (g)	HC (g)	GL (g)	deionized water (g)	PHG concentration
PHG-A	PHG-A10	28.6	60	20	891.4	10%
	PHG-A20	28.6	60	20	391.4	20%
	PHG-A30	28.6	60	20	224.7	30%
PHG-B	PHG-B10	57.1	40	20	882.9	10%
	PHG-B20	57.1	40	20	382.9	20%
	PHG-B30	57.1	40	20	216.2	30%
PHG-C	PHG-C10	85.7	20	20	874.3	10%
	PHG-C20	85.7	20	20	374.3	20%
	PHG-C30	85.7	20	20	207.6	30%

Preparation of IFR PHGs. The flame retardant solution was prepared by dissolving a flame retardant using a stirring method. Based on the different proportions of biomass-derived PA, HC, and GL (1:3:1, 2:2:1, and 3:1:1, calculated by anhydrous PA), three types of IFRs (PHG-A, PHG-B, and PHG-C) were prepared. Using deionized water as the solvent, the three flame retardants were prepared with 10, 20, and 30% aqueous solutions to form PHG-A, PHG-B, and PHG-C, respectively (combining anhydrous PA, HC, and GL). Table 3 lists the samples and dosages of each component.

Preparation of Flame Retardant Wood (PHG/Wood). The poplar flat-sawn board was cut into 100 × 10 × 10 and 100 × 100 × 5 mm subsamples and then heated to 103 °C until the weight of each sample was stable. Full cell process impregnation was then conducted at 20 °C. For this, the samples were immersed in containers with different concentrations of PHG (Table 3) and placed into a vacuum-pressurized dipping tank. The equipment was started, and a vacuum was created at 0.1 MPa, which was maintained for 30 min (step 1). The setup was then pressurized to 1.0 MPa and maintained for 24 h (step 2), after which the vacuum was reduced back to 0.1 MPa and held for 30 min (step 3). Finally, the samples were removed, and their surfaces were cleaned with deionized water. The samples were then dried in an oven at 103 °C until the weight was stable. The phosphate groups in PA react with the hydroxyl groups in cellulose,[21] lignin, and hemicellulose, thus combining PHG with the wood to form the prepared "PHG/wood" samples (Figure 8).

Characterization. The LOI test was conducted according to ASTM D 2863−17 (JF-4, Nanjing Jiangning Analytical Instrument Co. Ltd.). All samples had dimensions of 100 × 10 × 10 mm. FTIR spectroscopy was used to characterize the molecular structure of the samples using a Nicolet 5700 FT-IR spectrometer with KBr compression. The resolution of the FTIR spectrometer was 4 cm^{-1}, and the spectral range was 400−4000 cm^{-1}. The surface morphologies of all samples and their char residues were observed by field-emission scanning electron microscopy (FE-SEM) (model SU8010, Hitachi) combined with an energy-dispersive X-ray (EDX) detector. The structures of the samples before and after heating were observed using a digital microscope in transmission mode (VHX-6000, KEYENCE, Japan).

Fourier transform infrared spectroscopy−thermogravimetric analysis (FTIR-TGA) curves were obtained, and thermogravi-

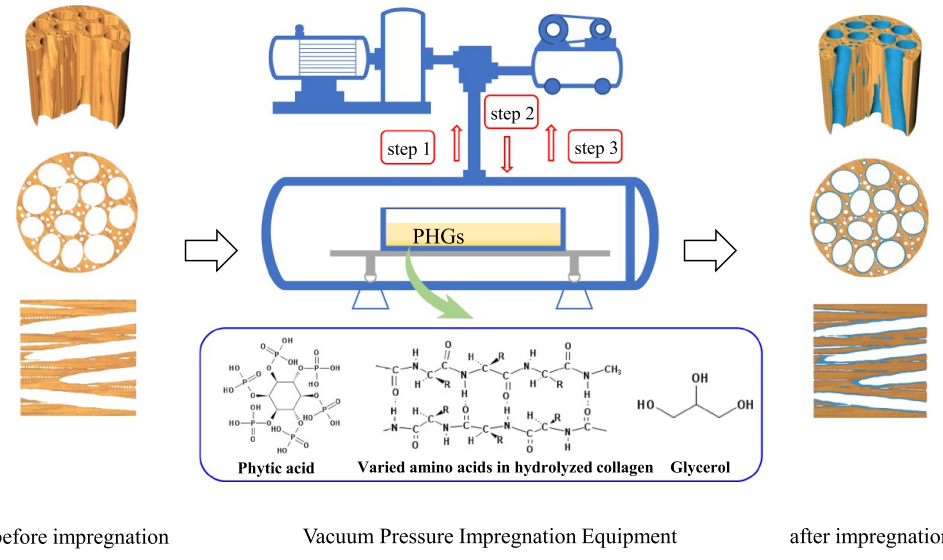

Figure 8. General process schematic for the preparation of impregnated PHG/wood samples.

https://dx.doi.org/10.1021/acsomega.0c05778
ACS Omega 2021, 6, 3921−3930

metric analysis (TGA) was performed using a TG analyzer (NETZSCH TG 209F1 Libra) equipped with an FTIR between 30 and 800 °C with a linear heating rate of 10 °C min^{-1} under a N flow of 10 mL/min. The spectra were recorded between 600 and 4000 cm^{-1} with an accumulation of eight scans and an optical resolution of 4 cm^{-1}. The weight of each sample was approximately 10 mg.

The cone calorimetry tests (CONE) were conducted in a Fire Testing Technology (FTT) apparatus according to the standard ASTM E1354-17 under an irradiative heat flux of 50 kW/m^2 with a horizontal configuration. All samples had dimensions of 100 × 100 × 5 mm. Finally, Raman spectroscopy (Renishaw invia, U.K.) was used to measure the graphitization of C residues at room temperature with a scanning range of 100−3200 cm^{-1} under a 532 nm He−Ne laser line.

AUTHOR INFORMATION

Corresponding Author

Peng Jiang − *Chinese Academy of Forestry, Research Institute of Wood Industry, 100091 Beijing, China;* orcid.org/0000-0002-5076-0943; Email: jiangpeng@caf.ac.cn

Authors

Luming Li − *Chinese Academy of Forestry, Research Institute of Wood Industry, 100091 Beijing, China*

Zhilin Chen − *Chinese Academy of Forestry, Research Institute of Wood Industry, 100091 Beijing, China*

Jinhan Lu − *Chinese Academy of Forestry, Research Institute of Wood Industry, 100091 Beijing, China*

Ming Wei − *Shangdong Xingang Enterprise Group Co., 276002 Linyi, China*

Yuxiang Huang − *Chinese Academy of Forestry, Research Institute of Wood Industry, 100091 Beijing, China*

Complete contact information is available at: https://pubs.acs.org/10.1021/acsomega.0c05778

Notes

The authors declare no competing financial interest.

ACKNOWLEDGMENTS

The authors wish to thank the Key R&D Program of China (grant no. 2017YFD0601106) and the Key R&D Program of Shandong Province (grant no. 2019JZZY010305) for their financial contributions.

REFERENCES

(1) Lowden, L.; Hull, T. Flammability behaviour of wood and a review of the methods for its reduction. *Fire Sci. Rev.* **2013**, *2*, 4.

(2) Gao, M.; Sun, C. Y.; Wang, C. X. Thermal degradation of wood treated with flame retardants. *J. Therm. Anal. Calorim.* **2006**, *85*, 765−769.

(3) Seo, H. J.; Kim, S.; Huh, W.; Park, K.-W.; Lee, D. R.; Son, D. W.; Kim, Y.-S. Enhancing the flame-retardant performance of wood-based materials using carbon-based materials. *J. Therm. Anal. Calorim.* **2015**, *123*, 1935−1942.

(4) Liao, S. F.; Deng, C.; Huang, S. C.; Cao, J. Y.; Wang, Y. Z. An efficient halogen-free flame retardant for polyethylene: piperazine-modified ammonium polyphosphates with different structures. *Chin. J. Polym. Sci.* **2016**, *34*, 1339−1353.

(5) Abou-Okeil, A.; El-Sawy, S. M.; Abdel-Mohdy, F. A. Flame retardant cotton fabrics treated with organophosphorus polymer. *Carbohydr. Polym.* **2013**, *92*, 2293−2298.

(6) Nabipour, H.; Wang, X.; Song, L.; Hu, Y. A fully bio-based coating made from alginate, chitosan and hydroxyapatite for protecting flexible polyurethane foam from fire. *Carbohydr. Polym.* **2020**, *246*, 116641.

(7) Ma, H.-X.; Li, J.-J.; Qiu, J.-J.; Liu, Y.; Liu, C.-M. Renewable cardanol-based star-shaped prepolymer containing a phosphazene core as a potential biobased green fire-retardant coating. *ACS Sustainable Chem. Eng.* **2017**, *5*, 350−359.

(8) Aqlibous, A.; Tretsiakova-Mcnally, S.; Fateh, T. Waterborne Intumescent Coatings Containing Industrial and Bio-Fillers for Fire Protection of Timber Materials. *Polymer* **2020**, *12*, 757.

(9) Camino, G.; Costa, L.; Martinasso, G. Intumescent fire-retardant systems. *Polym. Degrad. Stab.* **1989**, *23*, 359−376.

(10) Lu, J.; Jiang, P.; Chen, Z.; Li, L.; Huang, Y. Flame retardancy, thermal stability, and hygroscopicity of wood materials modified with melamine and amino trimethylene phosphonic acid. *Constr. Build. Mater.* **2020**, 121042.

(11) Graf, E. Application of phytic acid. *J. Am. Oil Chem. Soc.* **1983**, *60*, 1861−1867.

(12) Alongi, J.; Malucelli, G. Thermal Degradation of Cellulose and Cellulosic Substrates. *Reactions and Mechanisms in Thermal Analysis of Advanced Materials*, Tiwari, A.; Raj, B. (Eds.) Wiley Scrivener Publisher: Hoboken, NJ, USA, 2015; pp. 301−332.

(13) Liu, X.; Zhang, Q.; Peng, B.; Ren, Y.; Cheng, B.; Ding, C.; Su, X.; He, J.; Lin, S. Flame retardant cellulosic fabrics via layer-by-layer self-assembly double coating with egg white protein and phytic acid. *J. Cleaner Prod.* **2020**, *243*, 118641.

(14) Barbalini, M.; Bartoli, M.; Tagliaferro, A.; Malucelli, G. Phytic Acid and Biochar: An Effective All Bio-Sourced Flame Retardant Formulation for Cotton Fabrics. *Polymer* **2020**, *12*, 811.

(15) Cheng, X.-W.; Guan, J.-P.; Kiekens, P.; Yang, X.-H.; Tang, R.-C. Preparation and evaluation of an eco-friendly, reactive, and phytic acid-based flame retardant for wool. *React. Funct. Polym.* **2019**, *134*, 58−66.

(16) Shi, X.; Jiang, S.; Hu, Y.; Peng, X.; Yang, H.; Qian, X. Phosphorylated chitosan-cobalt complex: A novel green flame retardant for polylactic acid. *Polym. Adv. Technol.* **2018**, *29*, 860−866.

(17) Fang, F.; Huo, S.; Shen, H.; Ran, S.; Wang, H.; Song, P.; Fang, Z. A bio-based ionic complex with different oxidation states of phosphorus for reducing flammability and smoke release of epoxy resins. *Compos. Commun.* **2020**, *17*, 104−108.

(18) Boccafoschi, F.; Habermehl, J.; Vesentini, S.; Mantovani, D. Biological performances of collagen-based scaffolds for vascular tissue engineering. *Biomaterials* **2005**, *26*, 7410−7417.

(19) Lee, C. H.; Singla, A.; Lee, Y. Biomedical applications of collagen. *Int. J. Pharm.* **2001**, *221*, 1−22.

(20) Costes, L.; Laoutid, F.; Brohez, S.; Dubois, P. Bio-based flame retardants: When nature meets fire protection. *Mater. Sci. Engin.: R: Rep.* **2017**, *117*, 1−25.

(21) Liu, X.-H.; Zhang, Q.-Y.; Cheng, B.-W.; Ren, Y.-L.; Zhang, Y.-G.; Ding, C. Durable flame retardant cellulosic fibers modified with novel, facile and efficient phytic acid-based finishing agent. *Cellulose* **2018**, *25*, 799−811.

(22) Dong, Y.; Yan, Y.; Wang, K.; Li, J.; Zhang, S.; Xia, C.; Shi, S. Q.; Cai, L. Improvement of water resistance, dimensional stability, and mechanical properties of poplar wood by rosin impregnation. *Eur. J. Wood Wood Prod.* **2016**, *74*, 177−184.

(23) Carran, R. S.; Ghosh, A.; Dyer, J. M. The effects of zeolite molecular sieve based surface treatments on the properties of wool fabrics. *Appl. Surf. Sci.* **2013**, *287*, 467−472.

(24) Yin, W.; Chen, L.; Lu, F.; et al. Mechanically robust, flame-retardant poly (lactic acid) biocomposites via combining cellulose nanofibers and ammonium polyphosphate. *ACS Omega* **2018**, *3*, 5615−5626.

(25) Jiang, G.; Qiao, J.; Hong, F. Application of phosphoric acid and phytic acid-doped bacterial cellulose as novel proton-conducting membranes to PEMFC. *Int. J. Hydrogen Energy* **2012**, *37*, 9182−9192.

https://dx.doi.org/10.1021/acsomega.0c05778
ACS Omega 2021, 6, 3921−3930

(26) Barone, J. R.; Arikan, O. Composting and biodegradation of thermally processed feather keratin polymer. *Polym. Degrad. Stab.* **2007**, *92*, 859−867.
(27) Wu, Y.; Zhang, S.; Ren, Z.; et al. Flame retardant properties of phytic acid and melamine treated wood. *Journal of Beijing Forestry University* **2020**, *42*, 155−161.
(28) Qian, W.; Li, X. Z.; Wu, Z.-P.; Liu, Y.-Z.; Fang, C.-C.; Meng, W. Formulation of Intumescent Flame Retardant Coatings Containing Natural-Based Tea Saponin. *J. Agri. Food Chem.* **2015**, *63*, 2782−2788.
(29) Shang, S.; Yuan, B.; Sun, Y.; Chen, G.; Huang, C.; Yu, B.; He, S.; Dai, H.; Chen, X. Facile preparation of layered melamine-phytate flame retardant via supramolecular self-assembly technology. *J. Colloid Interface Sci.* **2019**, *553*, 364−371.
(30) Fu, Q.; Medina, L.; Li, Y.; Carosio, F.; Hajian, A.; Berglund, L. A. Nanostructured Wood Hybrids for Fire-Retardancy Prepared by Clay Impregnation into the Cell Wall. *ACS Appl. Mater. Interfaces* **2017**, *9*, 36154−36163.
(31) Slopiecka, K.; Bartocci, P.; Fantozzi, F. Thermogravimetric analysis and kinetic study of poplar wood pyrolysis. *Appl. Energy.* **2012**, *97*, 491−497.
(32) Gasparovic, L.; Korenova, Z.; Jelemensky, L. Kinetic study of wood chips decomposition by TGA. *Chem. Pap.* **2010**, *64*, 174−181.
(33) Huang, G.; Chen, W.; Wu, T. Multifunctional graphene-based nano-additives toward high-performance polymer nanocomposites with enhanced mechanical, thermal, flame retardancy and smoke suppressive properties. *Chem. Eng. J.* **2020**, 127590.
(34) Cheng, X.-W.; Liang, C.-X.; Guan, J.-P.; Yang, X.-H.; Tang, R.-C. Flame retardant and hydrophobic properties of novel sol-gel derived phytic acid/silica hybrid organic-inorganic coatings for silk fabric. *Appl. Surf. Sci.* **2018**, *427*, 69−80.
(35) Bachtiar, E. V.; Kurkowiak, K.; Yan, L.; Kasal, B.; Kolb, T. Thermal Stability, Fire Performance, and Mechanical Properties of Natural Fibre Fabric-Reinforced Polymer Composites with Different Fire Retardants. *Polymer* **2019**, *11*, 699.
(36) Brischke, C.; Welzbacher, C. R.; Brandt, K.; Rapp, A. O. Quality control of thermally modified timber: Interrelationship between heat treatment intensities and CIE L*a*b* color data on homogenized wood samples. *Holzforschung* **2007**, *61*, 19−22.
(37) Yang, H.; Yu, B.; Xu, X.; et al. Lignin-derived bio-based flame retardants toward high-performance sustainable polymeric materials. *Green Chem.* **2020**, *22*, 2129−2161.
(38) Xiong, Z.; Zhang, Y.; Du, X.; Song, P.; Fang, Z. Green and Scalable Fabrication of Core−Shell Biobased Flame Retardants for Reducing Flammability of Polylactic Acid. *ACS Sustainable Chem. Eng.* **2019**, *7*, 8954−8963.
(39) Sun, Y.; Sun, S.; Chen, L.; Liu, L.; Song, P.; Li, W.; Yu, Y.; Fengzhu, L.; Qian, J.; Wang, H. Flame retardant and mechanically tough poly(lactic acid) biocomposites via combining ammonia polyphosphate and polyethylene glycol. *Compos. Commun.* **2017**, *6*, 1−5.
(40) Xue, Y.; Shen, M.; Zheng, Y.; Tao, W.; Han, Y.; Li, W.; Song, P.; Wang, H. One-pot scalable fabrication of an oligomeric phosphoramide towards high-performance flame retardant polylactic acid with a submicron-grained structure. *Composites, Part B* **2020**, *183*, 107695.
(41) Li, W.-X.; Zhang, H.-J.; Hu, X.-P.; Yang, W.-X.; Cheng, Z.; Xie, C.-Q. Highly efficient replacement of traditional intumescent flame retardants in polypropylene by manganese ions doped melamine phytate nanosheets. *J. Hazard. Mater.* **2020**, *398*, 123001.
(42) Yin, S.; Ren, X.; Lian, P.; Zhu, Y.; Mei, Y. Synergistic effects of black phosphorus/boron nitride nanosheets on enhancing the flame-retardant properties of waterborne polyurethane and its flame-retardant mechanism. *Polymer* **2020**, *12*, 1487.
(43) Xue, Y.; Feng, J.; Huo, S.; et al. Polyphosphoramide-intercalated MXene for simultaneously enhancing thermal stability, flame retardancy and mechanical properties of polylactide. *Chem. Eng. J.* **2020**, 125336.
(44) Zhang, Z.; Li, X.; Ma, Z.; Ning, H.; Zhang, D.; Wang, Y. A facile and green strategy to simultaneously enhance the flame retardant and mechanical properties of poly(vinyl alcohol) by introduction of a bio-based polyelectrolyte complex formed by chitosan and phytic acid. *Dalton Trans.* **2020**, *49*, 11226−11237.
(45) Xing, C.-Y.; Zeng, S.-L.; Qi, S.-K.; Jiang, M.-J.; Xu, L.; Chen, L.; Zhang, S.; Li, B.-J. Poly (vinyl alcohol)/β-Cyclodextrin Composite Fiber with Good Flame Retardant and Super-Smoke Suppression Properties. *Polymer* **2020**, *12*, 1078.
(46) He, W.; Song, P.; Yu, B.; Fang, Z.; Wang, H. Flame retardant polymeric nanocomposites through the combination of nanomaterials and conventional flame retardants. *Prog. Mater. Sci.* **2020**, 100687.

https://dx.doi.org/10.1021/acsomega.0c05778
ACS Omega 2021, 6, 3921−3930